Crossref

DOI: 10.31643/2027/6445.16
Earth and Planetary Sciences: Earth-Surface Processes

Redistribution of rock pressure and deformation of the rock mass in the Karaganda coal basin

***Mussin R.A., Akhmatnurov D.R., Zamaliyev N.M.**

NPJSC Abylkas Saginov Karaganda Technical University, Karaganda, Kazakhstan

** Corresponding author email: r.a.mussin@mail.ru*

Received: *September 25, 2025*
Peer-reviewed: *October 2, 2025*
Accepted: *November 18, 2025*

ABSTRACT

The study examines the redistribution of rock pressure and associated deformation processes in the Karaganda Coal Basin. It focuses on the geometry and parameters of the abutment, unloading, and disintegration zones around underground workings, and on their influence on gas-dynamic phenomena. The methodological basis combines a critical review of current geomechanical models, calculation–graphic nomograms for estimating zone width as a function of mining depth and seam thickness, and schematic construction of high-stress regions from the boundaries of the goaf at limiting angles of 75–90°. It is shown that, with increasing depth up to about 500 m, the zone configuration becomes wedge-shaped with a tendency to narrow downward, while increasing seam thickness expands the affected areas. Lithology controls the localization of hazardous zones: weakly bedded argillites and siltstones accelerate loosening and loss of stiffness, whereas stronger sandstones form dome-like stress concentrations with elevated likelihood of sudden outbursts and rockbursts. As a verification case, an episode of a sudden coal-and-gas outburst was analyzed. The observed failure boundaries are consistent with the calculated wedge-shaped high-stress zone, supporting the validity of the chosen approach within the stated assumptions. The practical significance lies in refining threshold conditions that trigger mandatory comprehensive forecasting at depths exceeding ~400 m, justifying regular instrumental monitoring to validate calculations, and adjusting barrier-pillar parameters about seam thickness and depth. The findings can be applied to the planning and safe execution of longwall and development operations under outburst-prone conditions.

Keywords: abutment pressure, destressed zones, disintegration, mining depth, seam thickness, lithology.

Information about authors:

Mussin Ravil Altavovich	*PhD, Acting Associate Prof., NPJSC Abylkas Saginov Karaganda Technical University, Karaganda, Kazakhstan. Email: R.A.Mussin@mail.ru; ORCID ID: https://orcid.org/0000-0002-1206-6889*
Akhmatnurov Denis Ramilievich	*PhD, Head of Laboratory, NPJSC Abylkas Saginov Karaganda Technical University, Karaganda, Kazakhstan. Email: d.akhmatnurov@gmail.com; ORCID ID: https://orcid.org/0000-0001-9485-3669*
Zamaliyev Nail Mansurovich	*PhD, Associate Professor, NPJSC Abylkas Saginov Karaganda Technical University, Karaganda, Kazakhstan. Email: nailzamaliev@mail.ru; ORCID ID: https://orcid.org/0000-0003-0628-2654*

Introduction

Redistribution of rock pressure within the host rock mass is a core subject of mining geomechanics and directly governs the safety and operational stability of underground workings. Disturbance of the natural stress field during excavation generates local stress concentrators and zones of intense deformation and failure. These responses are systematic and manifest as a spectrum of complications ranging from loss of support capacity and instability of the excavation perimeter to sudden coal-and-gas outbursts and rockbursts [[1], [2], [3]]. The issue is particularly acute in coal basins that combine large depth ranges with high gas content. In the Karaganda Coal Basin, this constitutes a primary risk factor: production commonly proceeds at depths of ~400–600 m and greater, where the in-situ stress level approaches critical thresholds for several lithotypes and structural settings [4]. Coupled with the elevated methane potential of the seams, this increases the likelihood of dynamic phenomena—such as outbursts, roof/floor collapses, and rockbursts. Operational records and research indicate that 40–60 % of complications during longwall and development operations are directly associated with stress redistribution [[5], [6]]. The hazardous processes are hierarchical: local plastic deformation at the excavation boundary rapidly propagates to the scale of the rock mass, modifying the stress–strain state and permeability. Adjacent to the face, the abutment-pressure zone develops with elevated principal stresses; in the destressed zone, fracturing and disintegration progress, degrading stability, altering filtration regimes, and enhancing gas release. At the surface, these changes drive secondary deformations—subsidence, tensile cracking, and plan-position disturbance of infrastructure [[7], [8], [9]]. Lithological control is pivotal: weakly bedded argillites and siltstones accelerate yielding and loosening, whereas thick sandstone packages may form dome-like stress concentrations with heightened risk of dynamic events.

The practical framework requires a verifiable forecast of the configuration and parameters of influence zones, accounting for mining depth (H), seam thickness (m), structural disturbance, and the initial lateral stress coefficient K_0. Computational assessments should employ calibrated numerical models constrained by in-situ data: excavation convergence, ground-penetrating radar/ultrasonic surveys, acoustic-emission indicators, borehole logging, and stress measurements. On both longwall and development panels, continuous operational monitoring is warranted, including load cells and instrumented rock bolts, vibrating-wire gauges and fixed-point convergence meters, acoustic-emission and microseismic stations, and routine gas monitoring. Comparing deformation rates with trends in acoustic activity and gas emission enables timely identification of transitions to unstable regimes.

Engineering decisions must be explicitly tied to the mapped zones of influence: adjustment of support schemes, dimensions, and placement of barrier/chain pillars, extraction sequencing, face advance rate, and degasification regimes. For depths >400–500 m, it is advisable to adopt threshold criteria for switching to reinforced support and enhanced monitoring, and to apply refined nomograms of abutment-zone width that incorporate H, m, and rock properties. Without regular instrumental validation of models and adaptive updates to support designs, achieving the required levels of safety and reliability is not feasible; the integrated cycle "model → measurement → correction" is what sustains excavation stability and reduces the probability of sudden dynamic manifestations under the conditions characteristic of the Karaganda Coal Basin. Long-term accident statistics from Karaganda Coal Basin mines underscore the need for continual improvement in occupational safety practices and roadway stability management. At depths exceeding 500 m, conventional schemes for predicting rock-pressure zones lack sufficient sensitivity to heterogeneity and anisotropy of the rock mass, increasing the likelihood of suboptimal design decisions; refined, verifiable modeling and analysis methods are therefore required [[10], [11]]. A key applied task is the correct delineation of high-stress zones emanating from the edges of the goaf, since their geometry governs the serviceability of pillars and the longevity of workings left in place. Geomechanical models enable advanced estimation of the width and depth of influence zones, their linkage to longwall and development parameters, and timely adjustments to support designs. Field and desk studies indicate that deformation and failure foci are predominantly localized in coal seams overlain by weakly bedded argillites and siltstones, reinforcing the need to account comprehensively for lithological structure. Conversely, strong sandstones in the roof or floor promote dome-shaped stress concentrations and elevate the risk of sudden dynamic events. In practice, this manifests as perimeter deformation with spalling and crushing of supports and consequential ventilation disturbances, episodes of sudden coal-and-gas outbursts once critical stress thresholds are reached, rockbursts in tectonically disturbed zones at depths greater than 500 m, and roof collapses with floor heave that complicate longwall operations. Collectively, these factors reduce productivity and pose significant hazards to personnel; industry data indicate that outbursts and roof falls remain among the leading causes of accidents in Kazakhstan's coal mines.

Article Objective. Systematizing data on rock-pressure influence zones and their structural features is a necessary step toward developing effective methods for forecasting and preventing accident scenarios. Theory, experimental studies, and operational observations consistently show that characteristic zones form around the goaf: an abutment-pressure zone, a destressed (unloading) zone, a zone of complete disintegration, and a zone of secondary movements. Understanding their spatial configuration and parameters improves forecast accuracy and the defensibility of design choices. Accordingly, the objective of this article is to analyze and synthesize data on stress redistribution around underground workings, to demonstrate mechanisms of rock-mass failure using a documented coal-and-gas outburst, and to assess the applicability of these findings to the geological and operational conditions of the Karaganda Coal Basin.

Experimental part

Table 1 translates the qualitative stratigraphy into a compact input set for FEM/FDM initialization by listing density, stiffness, and strength contrasts for the principal layers together with reduced-shear behavior at bedding contacts; this allows the models to reproduce dome-like stress concentrations in stiff sandstone roofs and the weakening influence of laminated siltstone and argillite.

Table 1 - Condensed material and interface set for model initialization.

Series	H (m)	m (m)	K_0	Roof lithology	Reference L (m)
S1	400	1.0	0.7	siltstone/ argillite	L_0 (nomogram)
S2	600	2.0	0.8	laminated (weakened)	≈ 20 (per text)
S3	800	3.0	1.0	sandstone (stiff)	≈ 55 (per text)
S4	1000	4.0	1.1	faulted section	L_0; indicators check

Table 2 - Compact scenario grid for model–field comparison.

Layer / interface	ρ, t/m³	E, GPa	UCS, MPa	Purpose / note
Roof-1 (sandstone)	2.45–2.60	12–25	40–80	Stiff roof shaping dome-like stress fields
Roof-2 (siltstone)	2.40–2.55	6–12	15–40	Weaker laminated roof packages
Coal seam	1.30–1.45	1–3	4–12	Controls yielding (m = 1–4 m)
Floor (argillite)	2.40–2.55	3–8	10–25	Soft base influencing abutment width
Roof/seam contact	—	K_shear 50–150 MN/m	—	Reduced shear; μ 0.4–0.6; τ_max 1.0–2.5 MPa
Seam/floor contact	—	K_shear 50–120 MN/m	—	Reduced shear; μ 0.4–0.6; τ_max 0.8–2.0 MPa

These ranges operationalize the stratigraphic context into numerical inputs so simulations start from defensible stiffness/strength contrasts and reduced-shear contacts.

Table 2 organizes the model–field comparison into a concise scenario grid spanning depth (H), seam thickness (m) and lateral confinement (K_0) with lithology and contacts specified; L_0 from the nomogram is treated as the baseline, while the values already cited in the manuscript (≈20 m at H = 600 m and ≈55 m at H = 800 m) serve as anchors during interpretation.

The scenario grid defines which H–m–K_0 combinations are tested; the nomogram-based L_0 is the baseline, while the ≈20 m and ≈55 m figures already mentioned in the manuscript act as anchors for interpretation.

Redistribution of rock pressure within the host rock mass is a first-order subject of engineering analysis because it directly governs excavation stability and operational safety, especially under the conditions of the Karaganda Coal Basin. Disturbance of the natural stress field during drivage establishes a hierarchy of zones: at the excavation boundary, disintegration and intensive fracturing develop; outward from the contour, an abutment-pressure zone forms with principal stresses exceeding the in-situ level; farther out lies a destressed (unloading) zone characterized by reduced strength and increased jointing. Field observations show a rapid escalation from local plastic deformation at the boundary to rock-mass scale responses, accompanied by changes in the stress–strain state and in hydraulic and gas-dynamic regimes. Lithology is the controlling factor: weakly bedded argillites and siltstones accelerate loosening; thick, monolithic sandstones generate dome-shaped stress concentrations with elevated likelihood of dynamic manifestations; coal seams, combining low strength with high gas content, remain the most vulnerable element of the system. A schematic of the zoning and typical deformation forms is presented in Figure 1, which shows the initial and time-evolved excavation contours, weak and strong layers, the zone of complete failure, and tension-type termination cracks.

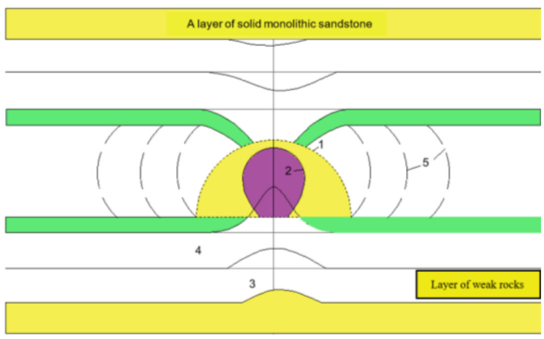

Figure 1 – Rock-mass failure deformation around an excavation with open support.
1-excavation contour immediately after drivage; 2-same after some time; 3-layers of weak rocks; 4-zone of completely crushed rock; 5-tension (termination) cracks; 6-layers of strong monolithic sandstone.

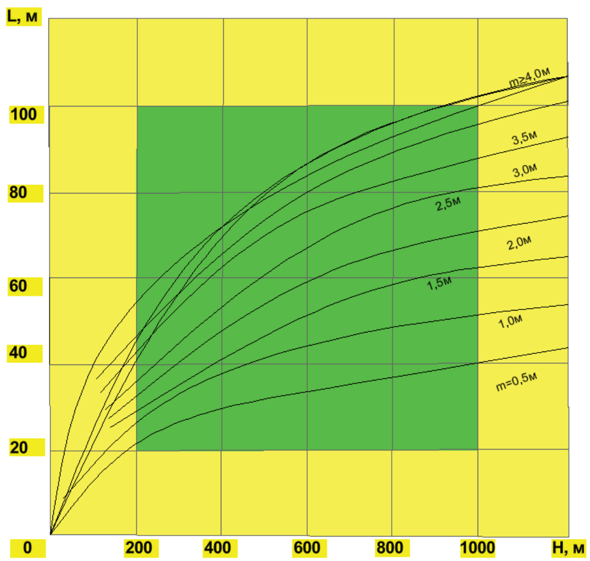

Figure 2 – Nomogram for determining the width of the abutment-pressure zone.
H – mining depth; m – seam thickness.

Quantitative evaluation is carried out using empirical–analytical relationships that link the width of the abutment-pressure zone (L) to mining depth (H), seam thickness (m), and the lateral stress coefficient (K_0). The nominal value L_0 is taken from the nomogram in Figure 2 for the pair (H, m), after which a correction model is applied:

$$L = L_0(H,m)\cdot k_{litho}\cdot k_{str}\cdot k_{K0}\cdot k_t \qquad (1)$$

where k_{litho} reflects lithology (sandstone 1.15–1.35; argillite/siltstone 0.85–0.95; heterogeneous section 1.00–1.10), k_{str} accounts for tectonic disturbance (fault zones 1.10–1.25; undisturbed strata 0.95–1.00), $k_{K0} \approx 0.9 + 0.4\ (K_0 - 0.7)$ for $0.6 \le K_0 \le 1.1$ describes the influence of lateral stress, and k_t = 1.00–1.10 is a time factor.

$$L_0(H, m) \approx am^{0,8}\ln(1+H/H_0) \qquad (2)$$

For rapid checks consistent with the nomogram in Figure 2, an approximation is used (with a = 26–28, H_0 = 90–110 m): at H = 1000 m and m = 4.0 m, L_0 is on the order of 55–60 m; at H = 400 m and m = 1.0 m, L_0 is about 12–14 m. These estimates are consistent with the family of calculated curves L(H) for m = 1–4 m in Figure 3.

Engineering application proceeds as follows. Specify H, m, and K_0, and describe lithology and structural disturbance; read L_0 from Figure 2, then apply the modifiers k_{litho}, k_{str}, k_{K0}, and k_t to obtain L. Next, verify by monitoring: excavation-contour convergence with acceleration exceeding 2–3 mm/day within 0.5·L; a twofold increase in acoustic/microseismic activity under steady ventilation; ground-penetrating radar and ultrasonic indications of local stiff inclusions; and a 30–50% increase in CH_4 flow rate and concentration at constant depression.

For a weakly bedded roof at H = 600 m, m = 2.0 m, K_0 = 0.8, and moderate disturbance, Figure 2 gives $L_0 \approx 22$ m; applying the modifiers k_{litho} = 0.9, k_{str} = 1.05, $k_{K0} \approx 0.96$, k_t = 1.05 yields $L \approx 20$ m. Recommended actions: reinforce support at the face, reduce the advance step, and drill lateral degasification holes 10–15 m long at a depression of 10–15 kPa.

For a strong sandstone roof at H = 800 m, m = 3.0 m, K_0 = 1.0, and local tectonics, Figure 2 gives $L_0 \approx 36$ m; with k_{litho} = 1.25, k_{str} = 1.15, $k_{K0} \approx 1.06$, k_t = 1.05, the result is $L \approx 55$ m. Recommended actions: increase the length of rock bolts and cable bolts, use yielding elements, reduce the face advance rate, and deploy an acoustic-emission station for early detection of transitions to unstable behavior.

Direct comparison of the nomogram in Figure 2 with the calculated families of curves in Figure 3 turns abutment-pressure assessment into a numerically guided decision process. Tying zone width to specific H, m, and K_0, while accounting for lithological–structural heterogeneity, provides a practical tool for adaptive adjustment of support designs and degasification schemes, maintaining roadway stability and reducing the likelihood of sudden dynamic events within the 200–1000 m depth range typical of the Karaganda Coal Basin.

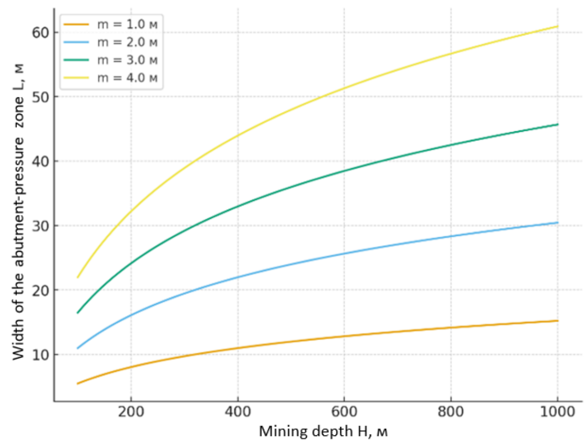

Figure 3 – Dependence of abutment-pressure zone width on depth for different seam thicknesses.

Analysis of the stress–strain state in the Karaganda Coal Basin shows that the boundaries of zones of elevated rock pressure dip at angles of 75–

90°, with formation depths of 250–500 m. Under these parameters, a characteristic wedge-shaped geometry develops, confining areas of maximum stress concentration. The construction is shown in Figure 4: cross-section (A) and along-strike section (B).

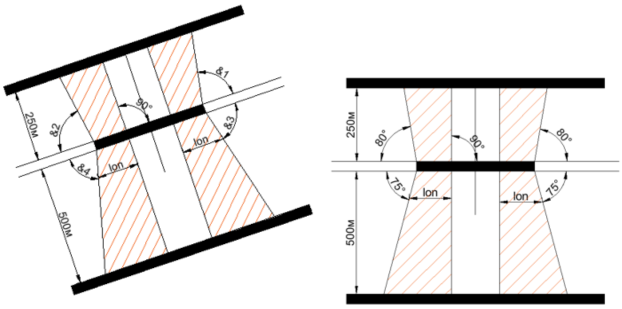

A B

Figure 4 – Scheme for constructing zones of elevated rock pressure
A – cross-section across strike, B – along-strike section.

The limiting boundaries are traced by projecting rays from the edges of the worked-out space and barrier pillars at angles of 75–90° to the horizontal. This angular range corresponds to the observed inclination of the stress-concentration front and is corroborated by mine observations and physical modeling. At depths of about 250 m, steeper fronts (80–90°) prevail; with increasing depth to 500 m, the zone acquires a pronounced wedge shape that narrows downward, and operating angles decrease to 75–80°. Thus, mining depth directly controls the spatial configuration of high rock-pressure fields.

Seam thickness exerts a decisive influence on the scale of the zones. For m ≤ 1.0 m, they remain compact and localized near the workings; for m ≥ 3.0–3.5 m, the zones become extensive, extend beyond nearby pillars, and may span several production blocks. This necessitates revising the width and geometry of barrier pillars, refining the extraction sequence, and repositioning development entries.

Mapping wedge-shaped zones of elevated rock pressure provides a targeted forecast of hazardous areas—zones prone to sudden outbursts, local collapses, and degradation of support capacity. Practical application of the scheme under Karaganda Basin conditions has confirmed its effectiveness for siting development workings and specifying barrier-pillar parameters tied to actual depth and seam thickness.

Continuing the discussion of elevated-pressure zones: in the immediate vicinity of the excavation, the stress gradients are maximal, and the subsequent evolution of the perimeter is determined there. The scheme in Figure 1 illustrates this dynamics: the initial contour (1) shortly after drivage passes through a brief period of relative stabilization and, under rock pressure and rock creep, transforms into the later contour (2). Between these states, a zone of complete failure (4) develops with a blocky mosaic and pronounced loosening. Along the tensile front, termination (tension) cracks (5) appear; their spacing and depth are governed by contrasts in deformation modulus and strength across bed contacts, the presence of weak interbeds, and the degree of natural disturbance.

Materials of differing strength behave fundamentally differently. In bedded argillites and siltstones, structural degradation proceeds rapidly: effective stiffness drops, roadway convergence accelerates, and support capacity is exhausted over short time frames. Under such conditions, an early switch to a reinforced support scheme is justified: increasing rock-bolt and cable-bolt length, reducing spacing, using yielding elements, installing protective pillars, and implementing advanced degasification. In monolithic sandstones, excavation geometry persists longer due to higher strength; however, dome-shaped stress concentrations develop in the roof and at contacts with weaker rocks. As critical levels are approached, short-lived bursts of acoustic activity are recorded, local high-stiffness zones are detected by ultrasonic and GPR surveys, and the stability margin collapses even under minor external perturbations. For such areas, combined support with pretension and controlled yielding is advisable, along with a reduced face-advance rate and continuous instrumented monitoring.

Time dependence is a key factor. Even where initial behavior is stable, within weeks a persistent trend of roof and floor displacement often emerges: the convergence rate increases within roughly 0.5·L of the abutment-pressure zone width, the share of low-frequency events in acoustic records grows, and gas emission rises steadily at constant ventilation depression. Joint interpretation of three independent monitoring channels—convergence measurements, acoustic/microseismic observations, and gas-dynamic parameters—allows early recognition of the sequence shown in Figure 1: the transition from the initial to the later contour via expansion of the complete-failure zone and development of tension cracks.

Design decisions under these conditions must be tightly linked to the map of lithological and structural heterogeneity. For weak strata, rational measures include densifying the support grid, increasing element length, extended degasification, and installing local protective pillars. For strong sandstone domains—lengthening bolts and cable bolts, using stiff-yielding inserts, and reducing the longwall advance rate. At contacts between rocks with contrasting properties, local reinforcements and limits on operational pauses are required to prevent self-propagation of the hazardous disintegration zones depicted in Figure 1.

Table 3 condenses the monitoring framework to three operational signals—convergence acceleration, growth of low-frequency acoustic activity, and CH_4 flow increase at constant depression—so that model outputs can be read against clear instability indicators; auxiliary channels such as support loads and GPR/ultrasonic scans remain within the narrative.

Table 3 - Core monitoring triad and thresholds used for operational interpretation.

Channel	Derived metric	Operational threshold
Convergence	acceleration d^2u/dt^2	≥ 2–3 mm/day within ~0.5·L
Acoustic/microseismic	share of low-frequency events	sustained increase
Gas flow (CH_4)	trend at fixed depression	30–50% rise

Note (Table 3). Each metric–threshold pair provides a bridge between stress/strain fields and observable underground behavior, guiding escalation to reinforced measures.

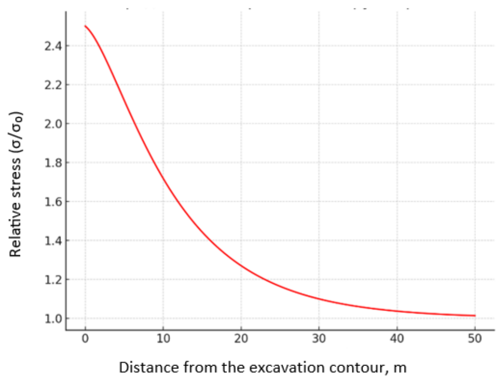

Figure 5 – Distribution of stresses around the excavation

Results and Discussion

Advancing the longwall face radically restructures the stress–strain state in the zone of development roadways and can lead to loss of their load-bearing capacity well before completion of seam extraction. The scheme in Figure 5 reflects a robust sequence: a roof caving dome forms, with its dimensions controlled by seam thickness, stiffness of the overlying strata, and the presence of weakly bedded interlayers; in the sidewalls, a squeezing zone develops, characterized by outward extrusion of the rock mass toward the goaf and opening of bedding/structure contacts; in the floor, a heave zone arises where vertical and horizontal stresses produce uplift and loosening of the rock. In the Karaganda Basin—where depths reach several hundreds of meters and gas content is high—these effects intensify: production observations indicate that the longwall front begins to measurably affect development entries already at an approach distance of 30–50 m, while the actual height of the caving dome and the widths of the squeezing and floor-heave zones may each reach tens of meters.

Engineering practice shows that the rate and amplitude of deformation are controlled by a combination of three factors: seam geometry (thickness, dip), lithologic contrast between roof and floor (monolithic sandstones versus argillites and siltstones), and operating regimes of the longwall (face advance rate, duration of technological pauses, ventilation depression, and degasification parameters). In weakly bedded strata, loosening accelerates, sidewall convergence increases, and support serviceability is lost early; with monolithic sandstones, excavation geometry persists longer, but dome-shaped stress concentrations accumulate in the roof and can trigger sudden collapses. As the face approaches, reliable indicators of transition to an unstable regime include acceleration of sidewall convergence to several millimeters per day within roughly one-half of the abutment-pressure zone width, a sustained increase in the count of low-frequency acoustic events, and growth of methane flow and concentration at constant ventilation depression. Joint interpretation of these three monitoring channels—geodetic and strain-gauge measurements, acoustic and microseismic records, and gas-dynamic control—enables timely refinement of the actual height of the caving dome and the boundaries of the squeezing and floor-heave zones shown in Figure 6.

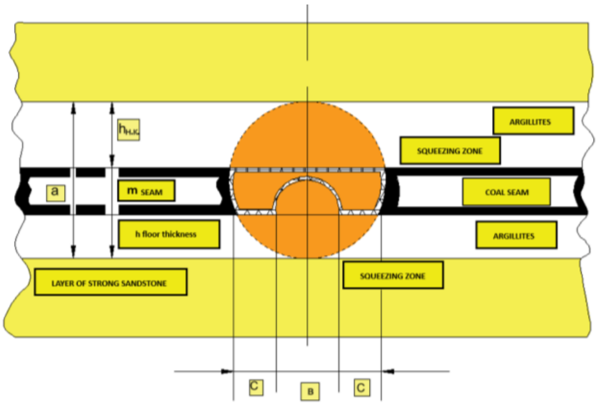

Figure 6 – Zone of potential rock-mass deformations around a development roadway under the influence of longwall operations

Design decisions should be directly grounded in such forecasts. For weak roofs and floors, appropriate measures include densifying the support pattern, increasing the length and pretension of rock bolts and cable bolts, using stiff-yielding elements, installing local protective pillars, and implementing advance degasification (lateral and inclined boreholes at a specified depression). For domains with monolithic sandstones, increase support capacity in combination with controlled yielding and a reduced face-advance step, and limit prolonged technological pauses to prevent self-amplification of the caving dome. Within the influence zone of longwall operations, development roadways should be treated as part of the overall stability system of the rock mass: their profile, support type, stand-off from the goaf, and degasification parameters must be revised as the face advances based on actual measurements rather than design assumptions alone. This "model — observe — adjust" regime provides the required stability margin and reduces the likelihood of sudden dynamic events at the depths and lithological conditions characteristic of the basin.

Redistribution of rock pressure. Advancing the longwall face radically restructures the stress–strain state in the zone of development entries and often leads to loss of load-bearing capacity long before seam extraction is completed. The scheme in Figure 6 illustrates a typical pattern. A roof caving dome forms; its height and span are governed by seam thickness, stiffness of the overlying strata, and the presence of weakly bedded interlayers. On the sidewalls, a squeezing zone develops, with the rock mass being extruded toward the goaf and bedding/structure contacts opening. In the floor, a heave zone forms where vertical and horizontal stresses cause uplift and loosening of the rock. This accelerates convergence growth and reduces the stability margin of the support.

Under Karaganda Basin conditions, the influence of the longwall front is amplified by mining depth and high gas content. Operational observations show that noticeable impacts on development roadways begin when the face approaches to 30–50 m. The roof caving zone and the squeezing and floor-heave zones can each extend for tens of meters. As the face advances, sidewall convergence rate increases, fracturing intensifies in argillites and siltstones, and gas emission rises at constant ventilation depression. Reliable indicators of transition to an unstable regime include acceleration of convergence to several millimeters per day within roughly half the abutment-pressure zone width, a sustained increase in low-frequency acoustic events, and growth of methane flow rate.

The rate and amplitude of deformations are controlled by three factor groups. The first is seam geometry, including thickness and dip. The second is contrast between roof and floor properties, where monolithic sandstones resist deformation longer while weakly bedded strata loosen more rapidly. The third is operating regime—face advance rate, duration of technological pauses, and degasification and ventilation parameters. Joint interpretation of three monitoring channels—convergence measurements, acoustic and microseismic records, and gas-dynamic control—allows refinement of the actual dome dimensions and the boundaries of the zones shown in Figure 7, and supports timely adjustment of decisions.

Design must be directly grounded in such monitoring. For weak roofs and floors, justified measures include densifying the support pattern; increasing the length and pretension of rock bolts and cable bolts; using stiff-yielding elements; installing local protective pillars; and implementing advance and side degasification at a specified depression. For domains with monolithic sandstones, it is advisable to combine higher support capacity with controlled yielding, reduce the face advance step, and limit prolonged technological pauses to prevent dome growth. Within the influence zone of longwall operations, development roadways should be treated as part of the overall stability system of the rock mass. Their profile, support type, stand-off from the goaf, and degasification parameters must be revised as the face advances, using actual measurements and threshold criteria. This model–observe–adjust algorithm provides the necessary stability margin and reduces the likelihood of sudden dynamic events at the depths and in the lithological conditions typical of the basin.

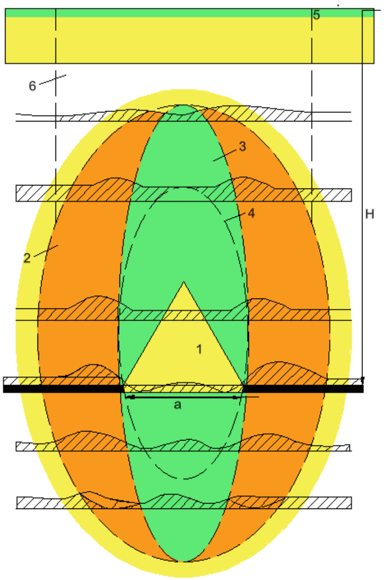

Figure 7 – Scheme of rock-pressure redistribution near a longwall working.
1 – area influenced by the working; 2 – abutment-pressure zone; 3 – boundary of the destressed zone; 4 – boundary of the protected zone; 5 – boundary of the zone of complete subsidence; 6 – zone of rock and ground-surface displacements arising from deformation of the rock mass within the abutment-pressure zone.

These zones do not act in isolation but as a single load-transfer framework: a stress change at the contour of a development or longwall working restructures the field above and below in the section, propagates upward to the roof, and can manifest at the ground surface as subsidence, crack opening, and terrain deformation. For the Karaganda Basin, the linkage between underground operations and surface deformation is confirmed by observations in areas of intensive mining: settlement peaks are recorded as the longwall face approaches, and their planform and amplitude are consistent with the configuration of the goaf and pillar parameters [[12], [13], [14], [15], [16], [17]].

From an engineering standpoint, pressure-redistribution zones constitute the skeleton of the rock mass geomechanical state and must be embedded in the design at all levels—from roadway alignment to the scheduling of block extraction. At the mine-field design stage it is advisable to construct a map of expected propagation angles and depths according to the scheme in Figure 4, specify calculated widths of the abutment-pressure and destressed zones, determine the minimum permissible distances between the goaf and development entries, and design protective pillars about their actual load-bearing capacity. In the technological part, this means choosing support type and spacing, face-advance rate, degasification regime, and limits on operational pauses in zones where a transition to unstable behavior is possible. In the operational part, it entails organizing continuous monitoring, including convergence measurements, acoustic–seismic observations, gas-dynamic measurements, and repeat surface geodetic surveys. Upon reaching threshold values, response measures are triggered—support reinforcement, denser bolt patterns, adjustment of the advance rate, local protective pillars, and modified degasification schemes.

This approach enables control of the entire system of zones from the face to the surface: local load redistribution at the working is promptly accounted for in roof and floor stability calculations, in assessing impacts on adjacent horizons, and in forecasting surface subsidence. Tying decisions to the scheme in Figure 4 and to in-situ measurements reduces the likelihood of sudden dynamic events and ensures the required safety level for seam extraction under the conditions of the Karaganda Coal Basin.

Field case. As an illustration, consider the sudden coal-and-gas outburst that occurred on 28 December 1976 in the manway at level +0 m of the Lenin Mine in the Karaganda Coal Basin. The incident took place in Seam D-6 at a depth of 411 m, with a roadway width of 6.0 m and a height of 3.25 m (see Figure 5).

According to the analysis, a zone of intense crushing and deformation formed in the coal seam adjacent to a tectonic disturbance near the outburst location. The character of the damaged zone (up to 5.0 m wide from the excavation contour) was accompanied by significant methane release. The gas-dynamic event was sharp and short-lived, consistent with the criteria of a sudden outburst, and with ground-control practice in longwall environments [[18], [19], [20]].

Comparison of the documented case with the calculated schemes of elevated rock-pressure zones (see Figure 6) showed agreement: the outburst area was localized within a wedge-shaped stress zone bounded by angles of 75–80° and situated immediately adjacent to the edge of the worked-out space. The accident thus confirmed the practical applicability of the pressure-zone construction methodology for forecasting the most hazardous areas, consistent with stress concentration concepts in rock mechanics and roadway support design.

Plan. Scale 1:500.

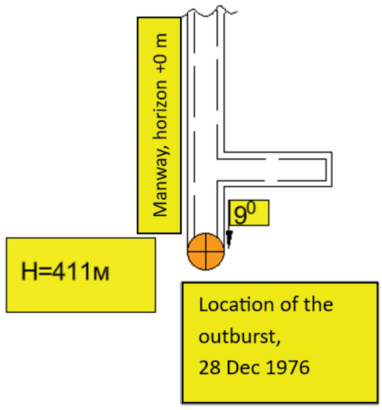

A

Dip section. Scale 1:200.

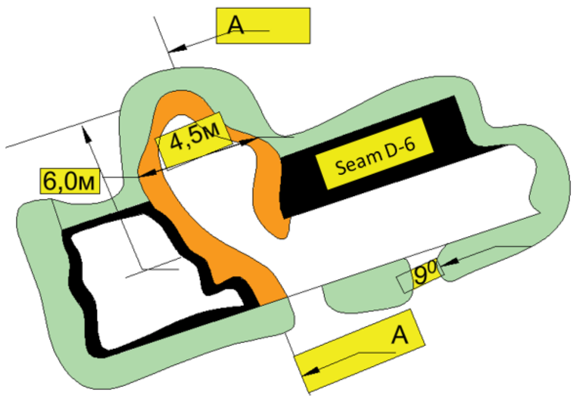

B

Strike section (A–A). Scale 1:100.

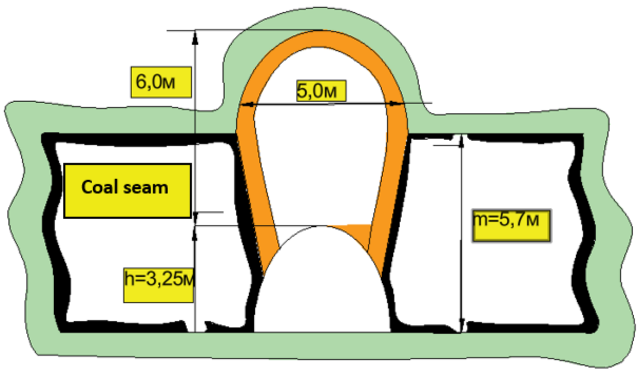

C

Figure 8 – Sketch of the sudden outburst site with elevated gas emission that occurred on 28 December 1976 in the manway at level +0 m of the Lenin Mine.

Comparison of the calculated schemes with in-situ observations confirms that the adopted zoning model for stress redistribution adequately represents rock-mass behavior in the Karaganda Coal Basin, aligning with established frameworks in rock mechanics and rock-mass classification. The system shows the highest sensitivity to three groups of risk factors. First, mining depth: once depths exceed roughly 400 m, rock-mass stress increases nonlinearly, consistent with the classic concepts of underground-excavation geomechanics by V. S. Kuznetsov and with the principles of rock-pressure control by V. P. Sakhno et al. In practice, this manifests as a rapid loss of stability margin in development and longwall roadways as they approach high-stress zones, a pattern well recognized in longwall and ground-control literature. Second, lithological structure: the association of coal seams with weak layers—argillites and siltstones—consistently produces zones of disintegration and accelerates loosening; this conclusion is supported by regional data on gas content and the structure of coal-bearing strata in the Karaganda Basin reported by M. A. Ermekov and by recent engineering studies on drivage and maintenance of cross-cuts by G. D. Tanekeyeva, E. A. Abeuov, D. R. Makhmudov, R. A. Mussin, and A. Yu. Balabas, and is consistent with rock-mass rating and Q-system perspectives on weak strata. Third, tectonic disturbance: faulted and crushed zones function as stress concentrators and are statistically correlated with sudden dynamic manifestations; this is emphasized in the work of V. S. Zaburdyaev on degasification parameters for high-productivity panels and is corroborated by calculation-instrumental solutions for stabilizing the mine floor by D. Akhmatnurov, N. Zamaliyev, R. Mussin, and co-authors, and by guidance on rockburst-prone conditions.

From a practical standpoint, the calculated boundaries of influence zones must be testable against measurable indicators. As stability limits are approached, the following are recorded: accelerated roadway convergence, a rise in low-frequency acoustic activity under constant ventilation depression, and a sustained increase in gas emission. Combined analysis of these time series refines the position of the abutment-pressure front, the boundaries of unloading, and the domain of complete disintegration. This approach aligns with current technological solutions for gas management and rock-mass deformation, including hydraulic flushing and hydraulic splitting for low-permeability coals (R. Zhang, C. Hao), consideration of swelling mechanisms and secondary deformations in complex geological settings (S. Y. Mu, Z. Ma), and synthesized observations of rock-mass behavior around roadways in deep mines (K. Skrzypkowski, W. Korzeniowski, J. Stasica). At the project stage this means specifying initial contours of influence zones and minimum offsets from the goaf as starting values subject to systematic refinement via monitoring; the switch to reinforced support and intensified degasification should be triggered by threshold values of observed parameters rather than by calendar schedules, in line with the logic of rock-pressure control set out by Kuznetsov and Sakhno, and by longwall/ground-control best practice.

The detailing of engineering measures is governed by lithological–structural conditions. In weakly bedded sequences with argillites and siltstones, justified actions include longer and pretensioned rock bolts and cable bolts, reduced spacing, use of stiff-yielding inserts, installation of local pillars, and advance degasification via lateral and inclined boreholes; the combined effect of these measures is reflected in modern publications on the geomechanical conditions of roadway drivage and maintenance, in technological solutions for intensifying gas drainage, and in standard references on ground control and roadway support. In domains dominated by monolithic sandstones—where roadway geometry persists longer but dome-shaped stress concentrations develop—it is advisable to combine higher support capacity with limits on the face advance rate and regulated technological pauses to prevent dome growth and brittle collapses; this strategy accords with the foundational principles of rock-pressure management in the classic sources and with synthesized evidence on rock-mass behavior in deep mines. Within zones influenced by tectonic structures, increasing ventilation depression to boost gas flow must be accompanied by continuous acoustic and deformation monitoring, since excessive unloading can hasten the transition to instability; this interrelation is discussed in detail in studies of degasification parameters for high-productivity panels and in work on stabilizing the working floor. Where applicable, proprietary support and damping solutions and protected technical designs can be referenced for implementation [[21, [22]].

Finally, the limits of applicability must be recognized. Linear construction of zone boundaries cannot capture the full heterogeneity of the section and the variability of contacts; the temporal component—creep, stress relaxation, and changes in filtration and gas-dynamic regime—can recon Figure conditions weeks to months after drivage or extraction. Consequently, calculated decisions must be accompanied by instrumental verification: GPR and ultrasonic surveys to detect local stiff inclusions, acoustic and microseismic measurements to capture transitions to instability, and repeat surface geodetic surveys in areas of expected subsidence. This “model—observe—adjust” regimen rests on the proven methodological foundations of Kuznetsov and Sakhno, is supported by regional gas-content and structural data from Ermekov, and is reinforced by contemporary engineering studies in geomechanics and degasification, ensuring the required stability margin and reducing the probability of sudden dynamic events at the depths and lithological–structural conditions characteristic of the Karaganda Coal Basin [[23], [24], [25], [26]].

Conclusions

To substantiate safe extraction of seams in the Karaganda Coal Basin, the rock mass must be treated not as a set of local boundary effects but as a coherent system of processes with a clear space–time structure. Calculations and in-situ observations show that an interlinked hierarchy of zones forms around underground workings: at the boundary lies the abutment-pressure zone with elevated principal stresses; farther out is an unloading zone with reduced strength and increased jointing; beyond it, a disintegration zone with loss of structural integrity; and farther still, a domain of secondary movements through which deformations propagate away from the working and upward through the section to the ground surface. The system is nonlinear: any change in one zone reorganizes adjacent zones and sets the dynamics of the entire stress field.

Combined analysis of calculated schemes and field data indicates that maximum risks localize near the edges of the worked-out space and protective pillars, where wedge-shaped stress-concentration fronts form at angles of about 75–90° to the horizontal. At depths around 250 m, steeper fronts (80–90°) prevail; by 500 m, the wedge narrows downward at 75–80°, defining areas of highest likelihood for brittle collapses and dynamic events. The geometry is validated in practice: the sudden outburst at the Lenin Mine (Seam D-6, 1976, depth 411 m) reproduced the calculated scenario—the observed failure boundaries coincided with the predicted wedge-shaped high-stress zone.

For design under basin conditions, the controlling factors remain lithological contrast, gas content, and tectonic disturbance. Bedded argillites and siltstones accelerate loosening and enlarge the disintegration domain; monolithic sandstones preserve roadway geometry longer but accumulate dome-shaped stress fields. High gas content lowers resistance to perturbations, while faulted and crushed zones act as stress concentrators and deformation conduits, sharply increasing the sensitivity of the rock mass as the longwall front approaches.

This leads to concrete engineering requirements. At depths above an indicative threshold of 400 m, a comprehensive geomechanical forecast is needed, with construction of wedge boundaries and estimation of influence-zone width for given depth and seam thickness. Operations should be accompanied by continuous instrumentation: convergence measurements, acoustic–microseismic monitoring, GPR/ultrasonic surveys of roof and floor, and real-time gas dynamics. Reliable indicators of an approach to instability include acceleration of convergence to several millimetres per day within roughly half the abutment-zone width, a sustained rise in low-frequency acoustic events, and increased methane flow/concentration at constant ventilation depression. Protective-pillar parameters should be adjusted for seam thickness, depth, and proximity to wedge zones; minimum sizes should be abandoned near faults. Support schemes must be adapted to actual influence-zone boundaries: increase bolt and cable-bolt length and pretension, tighten spacing, and employ stiff-yielding elements; in monolithic sandstones, combine higher load-bearing capacity with limits on face-advance rate and regulated pauses to prevent self-growth of a stress dome. To reduce outburst hazard, advance and lateral degasification at specified depressions, local relief workings, and controlled ventilation regimes are justified.

Organizationally, this is implemented as a strict "model — observe—adjust" cycle. Initial contours of influence zones set starting design values; as the face advances and monitoring data accrue, support type and spacing, pillar width and geometry, advance rate, and degasification parameters are refined. This regime provides the necessary stability margin for development and longwall roadways and lowers the probability of sudden dynamic events at the depths and under the lithological–structural conditions typical of the Karaganda Coal Basin.

Conflicts of interest. On behalf of all authors, the corresponding author states that there is no conflict of interest.

CRediT author statement: **R. Mussin**: Conceptualization, Methodology, Software, Data curation; **D. Akhmatnurov**: Writing draft preparation, Visualization, Investigation; **N. Zamaliyev:** Supervision, Software, Validation, Reviewing and Editing.

Acknowledgements. This research was carried out with the support of the Science Committee of the Ministry of Science and Higher Education of the Republic of Kazakhstan within the framework of program-targeted financing for the implementation of the scientific and scientific-technical program of the IRN BR28712407.

Cite this article as: Mussin RA, Akhmatnurov DR, Zamaliyev NM. Redistribution of rock pressure and deformation of the rock mass in the Karaganda coal basin. Kompleksnoe Ispolzovanie Mineralnogo Syra = Complex Use of Mineral Resources. 2027; 341(2):36-48. https://doi.org/10.31643/2027/6445.16

Қарағанды көмір бассейніндегі тау жыныстары қысымының және тау жыныстарының сілемінің деформациясының қайта таралуы

***Мусин Р.А., Ахматнуров Д.Р., Замалиев Н.М.**

КЕАҚ Әбілқас Сағынов атындағы Қарағанды техникалық университеті, Қарағанды, Қазақстан

Мақала келді: *25 қыркүйек 2025*
Сараптамадан өтті: *2 қазан 2025*
Қабылданды: *18 қараша 2025*

ТҮЙІНДЕМЕ

Бұл зерттеу Қарағанды көмір алабында жыныс сіләміндегі тау қысымының қайта бөлінуі мен соған ілеспе деформациялық үдерістерді қарастырады. Жер асты қазбаларының айналасындағы тірек қысымы, түсіру және ыдырау аймақтарының геометриясы мен параметрлері, сондай-ақ олардың газ-динамикалық құбылыстардың көріністеріне әсері қарастырылады. Әдістемелік негізге қолданылған геомеханикалық модельдерге сыни шолу, аймақтардың енін қабаттың тереңдігі мен қалыңдығына байланысты бағалауға арналған есептеу және графикалық номограммалар, сондай-ақ 75-90° шекті бұрыштарда өндірілген кеңістік шекараларынан кернеуі жоғары аймақтардың схемалық құрылысы кіреді. Игеру тереңдігі шамамен 500 м-ге дейін артқан кезде аймақтардың конфигурациясы төмен қарай тарылуға бейім сына тәрізді сипатқа ие болатыны анықталды; қабат қалыңдығының ұлғаюы әсер ету аймақтарының кеңеюіне әкеледі. Литологиялық бөлім қауіпті аймақтардың орналасуын бақылайды: әлсіз қабатты балшық тастар мен алевролиттер декомпрессияны жеделдетеді, ал күштірек құмтастар кенеттен атқылаулар мен тау жыныстарының жарылу ықтималдығы жоғарылайтын кернеу шоғырланған күмбез тәрізді аймақтарды құрайды. Тексеру мысалы ретінде көмір мен газдың кенеттен шығарындыларының бір эпизоды талданды. Нақты қирау шекараларын есептелген сына тәрізді кернеу аймағымен салыстыруға болады, бұл мәлімделген болжамдар шеңберінде таңдалған тәсілдің дұрыстығын растайды. Нәтижелердің практикалық маңыздылығы ~400 м-ден астам тереңдікте міндетті кешенді болжау үшін шекті шарттарды нақтылауда, есептеулерді тексеру үшін үнемі аспаптық бақылауды негіздеуде және қабаттардың қалыңдығы мен тереңдігін ескере отырып, қорғаныс тіректерінің параметрлерін түзетуде жатыр. Зерттеу нәтижелері қауіпті шығарындылар жағдайында тазалау және дайындық жұмыстарын жоспарлау және қауіпсіз жүргізу кезінде пайдаланылуы мүмкін.

Түйін сөздер: тірек қысымы, түсіру аймақтары, дезинтеграция, қазу тереңдігі, қабат қалыңдығы, литология.

Авторлар туралы ақпарат:

Мусин Равиль Альтавович — *PhD, қауымдастырылған профессор, КЕАҚ Әбілқас Сағынов атындағы Қарағанды техникалық университеті, Қарағанды, Қазақстан. Email: R.A.Mussin@mail.ru; ORCID ID: https://orcid.org/0000-0002-1206-6889*

Ахматнуров Денис Рамильевич — *PhD, зертхана жетекшісі, КЕАҚ Әбілқас Сағынов атындағы Қарағанды техникалық университеті, Қарағанды, Қазақстан. Email: d.akhmatnurov@gmail.com; ORCID ID: https://orcid.org/0000-0001-9485-3669*

Замалиев Наиль Мансурович — *PhD, қауымдастырылған профессор, КЕАҚ Әбілқас Сағынов атындағы Қарағанды техникалық университеті, Қарағанды, Қазақстан. Email: nailzamaliev@mail.ru; ORCID ID: https://orcid.org/0000-0003-0628-2654*

Перераспределение горного давления и деформации массива пород в условиях Карагандинского угольного бассейна

***Мусин Р.А., Ахматнуров Д.Р., Замалиев Н.М.**

НАО Карагандинский технический университет имени Абылкаса Сагинова, Караганда, Казахстан

Поступила: *25 сентября 2025*
Рецензирование: *2 октября 2025*
Принята в печать: *18 ноября 2025*

АННОТАЦИЯ

Работа посвящена анализу перераспределения горного давления и связанных с ним деформационных процессов в условиях Карагандинского угольного бассейна. Рассматриваются геометрия и параметры зон опорного давления, разгрузки и дезинтеграции вокруг подземных выработок, а также их влияние на проявления газодинамических явлений. Методическая основа включает критический обзор применяемых геомеханических моделей, расчетно-графические номограммы для оценки ширины зон как функций глубины залегания и мощности пласта, а также схемное построение областей повышенных напряжений от границ выработанного пространства под предельными углами 75–90°. Установлено, что при увеличении глубины разработки до порядка 500 м конфигурация зон приобретает клиновидный характер с тенденцией к сужению книзу; рост мощности пласта приводит к расширению областей влияния. Литологический разрез контролирует локализацию опасных зон: слабослоистые аргиллиты и алевролиты ускоряют разуплотнение, тогда как более прочные песчаники формируют куполообразные области концентрации напряжений с повышенной вероятностью внезапных выбросов и горных ударов. В качестве верификационного примера проанализирован эпизод внезапного выброса угля и газа. Фактические границы разрушения сопоставимы с расчетной клиновидной зоной повышенных напряжений, что подтверждает корректность выбранного подхода в пределах заявленных допущений. Практическая значимость результатов состоит в уточнении пороговых условий для обязательного комплексного прогноза на глубинах свыше ~400 м, в обосновании регулярного инструментального контроля для верификации расчетов и в корректировке параметров охранных целиков с учетом мощности пластов и глубины. Полученные выводы могут быть использованы при планировании и безопасном ведении очистных и подготовительных работ в выбросоопасных условиях.

Ключевые слова: опорное давление; зоны разгрузки; дезинтеграция; глубина разработки; мощность пласта; литология.

Информация об авторах:

Мусин Равиль Альтавович — *PhD, Ассоциированный профессор, НАО Карагандинский технический университет имени Абылкаса Сагинова, Караганда, Казахстан. Email: R.A.Mussin@mail.ru; ORCID ID: https://orcid.org/0000-0002-1206-6889*

Ахматнуров Денис Рамильевич	*PhD, руководитель лаборатории, НАО Карагандинский технический университет имени Абылкаса Сагинова, Караганда, Казахстан. Email: d.akhmatnurov@gmail.com; ORCID ID: https://orcid.org/0000-0001-9485-3669*
Замалиев Наиль Мансурович	*PhD, Ассоциированный профессор, НАО Карагандинский технический университет имени Абылкаса Сагинова, Караганда, Казахстан. Email: nailzamaliev@mail.ru; ORCID ID: https://orcid.org/0000-0003-0628-2654*

References

[1] Kuznetsov VS. Geomekhanika podzemnykh vyrabotok [Geomechanics of Underground Workings]. Moscow: Nedra. 1983, 256. (in Russ.).

[2] Nozhkin NV. Gidroraschlenenie (gidrorazryv) ugol'nykh plastov [Hydraulic Dissection (Hydraulic Fracturing) of Coal Seams]. Moscow: Gornaya Kniga. 1965, 214. (in Russ.).

[3] Sakhno VP, et al. Upravlenie gornym davleniem na ugol'nykh shakhtakh [Control of Rock Pressure in Coal Mines]. Donetsk: Donbass. 1990, 312. (in Russ.).

[4] Ermekov MA. Gazonosnost' uglenosnykh tolshch i gazovydelenie shakht Karagandinskogo basseina: avtoreferat dissertatsii doktora geologo-mineralogicheskikh nauk [Gas Content of Coal-Bearing Deposits and Gas Emission of Mines in the Karaganda Basin: Doctoral Dissertation Abstract. Geol.–Miner. Sci. Alma-Ata. 1963, 63. (in Russ.).

[5] Tanekeyeva GD, Abeuov EA, Makhmudov DR, Mussin RA, Balabas AYu. Issledovanie geomekhanicheskikh uslovii provedeniya i podderzhaniya kvershlagov [Study of Geomechanical Conditions for Driving and Maintaining Crosscut Mine Workings]. Ugol'. Coal. 2023; 2:31–33. (in Russ.). https://doi.org/10.18796/0041-5790-2023-2-31-33

[6] Airuni AT, et al. Formy svyazyvaniya metana s uglem [Forms of Methane Bonding with Coal]. Gorny Zhurnal (Mining Journal). 1990; 7:45–52. (in Russ.).

[7] Zaburdyaev VS. Parametry degazatsii v vysokoproizvoditel'nykh ochistnykh raionakh na nerazvedannykh shakhtnykh polyakh [Parameters of Degassing in High-Productivity Longwall Districts on Unexplored Mine Fields]. Bezopasnost' truda v promyshlennosti [Occupational Safety in Industry]. 2021; 2:63–68. (in Russ.).

[8] Akhmatnurov D, Zamaliyev N, Mussin R, Demin V, Ganyukov N, Zagórski K, Skrzypkowski K, Korzeniowski W, Stasica J. Optimization of reinforcement schemes for stabilizing the working floor in coal mines based on an assessment of its deformation state. Materials. 2025; 18(13):3094. https://doi.org/10.3390/ma18133094

[9] Zhang R, Hao C. Research on the development of hydraulic flushing caverns for gas extraction in soft, low-permeability tectonic coal seams in China. ACS Omega. 2022; 7(25):21615–21623. https://doi.org/10.1021/acsomega.2c01465

[10] Mu SY, Ma Z. Analysis of the mechanism of deformations and auxiliary technology for swelling of the rocky roadbed in deep complex geological conditions. Coal Mines. 2016; 47:95–98.

[11] Skrzypkowski K, Korzeniowski W, Stasica J. Rock mass behavior around roadways in deep mines. Archives of Mining Sciences. 2021; 66(4):679–696. https://doi.org/10.24425/ams.2021.139586

[12] Cai M, Kaiser PK. Numerical simulation of the rock-mass failure process at deep-level mines. International Journal of Rock Mechanics and Mining Sciences. 2018; 104:99–112.

[13] Lobanov NN. Dinamicheskie yavleniya na ugol'nykh shakhtakh [Dynamic Phenomena in Coal Mines]. Moscow: Nedra. 1987, 280. (in Russ.).

[14] Wu Q, Li X, Wang E. Numerical simulation of stress redistribution around coal-mining workings. International Journal of Mining Science and Technology. 2019; 29(2):243–251.

[15] Shabarov VV, Skrzypkowski K, Zamaliyev NM. Geomechanical problems of mining at large depths in the Karaganda Coal Basin. Mining of Mineral Deposits. 2023; 17(3):1–12.

[16] Sadchikov AV, Zamaliyev NM, Akhmatnurov DR, Mussin RA, Ganyukov NYu. Primenenie metodov marksheyder-sko-geofizicheskikh issledovanii dlya resheniya zadach geologii [Application of Mine-Geophysical Methods to Solving Problems of Geology]. Gorny informatsionno-analiticheskii byulleten' (Mining Informational and Analytical Bulletin). 2025; 6:109–124. (in Russ.).

[17] Hoek E, Brown ET. Practical estimates of rock-mass strength. International Journal of Rock Mechanics and Mining Sciences. 1997; 34(8):1165–1186. https://doi.org/10.1016/S1365-1609(97)80069-X

[18] Salamon MDG, Munro AH. A study of the strength of coal pillars. Journal of the South African Institute of Mining and Metallurgy. 1967; 68(2):55–67.

[19] Brady BHG, Brown ET. Rock Mechanics for Underground Mining. 4th ed. Heidelberg: Springer. 2013, 628. ISBN 978-94-007-7078-1.

[20] Peng SS. Longwall Mining. 3rd ed. Englewood, CO: Society for Mining, Metallurgy & Exploration. 2019, 621. ISBN 978-0-87335-445-3.

[21] Pat. 195044 KZ. Povyshenie bezopasnosti vedeniya gornykh rabot za schet uluchsheniya kachestva krepleniya [Improving the Safety of Mining Operations by Enhancing Support Quality]. Mussin RA, Balabas AYu, Doni DS, Alzhanova AM, Madiyarov TA, Dalibaev AZh, Kalmurzin EG, Kim RS. Opubl. 23.02.2023, 2. (in Russ.).

[22] Pat. 342325 KZ. Ustroystvo dlya gasheniya udarnoy volny [Device for Damping a Shock Wave]. Zamaliyev NM, Akhmatnurov DR, Mussin RA, Ganyukov NYu, Golik AV, Schmidt-Fedotova IM. Opubl. 23.01.2025, 1. (in Russ.).

[23] Barton N, Lien R, Lunde J. Engineering classification of rock masses for the design of tunnel support. Rock Mechanics. 1974; 6(4):189–236.

[24] Peng SS. Coal Mine Ground Control. 3rd ed. Morgantown: West Virginia University. 2008, 458.

[25] Kaiser PK, McCreath DR, Tannant DD. Canadian Rockburst Support Handbook. Sudbury, Ontario: Geomechanics Research Centre. 1996, 314.

[26] Whittaker BN, Reddish DJ. Subsidence: Occurrence, Prediction and Control. Amsterdam: Elsevier. 1989, 528.